Journal of Environmental Sciences Vol. 18, No. 1, pp. 69--75, 2006

ISSN 1001—0742
CN 11--2629/X

Article ID: 1001-0742(2006)01-0069-07 CLC number: X511; O657.32 Document code: A

Observation of atmospheric nitrous acid with DOAS in Beijing, China

QIN Min, XIE Pin-hua, LIU Wen-qing, LI Ang, DOU Ke, FANG Wu, LIU Jian-guo, ZHANG Wei-jun

(Key Laboratory of Environmental Optics and Technology, Anhui Institute of Optics and Fine Mechanics, Chinese Academy of Sciences, Hefei 230031, China. E-mail: mqin@aiofm.ac.cn)

Abstract: Measurements of nitrous acid (HONO) and nitrogen dioxide (NO_2) in Beijing City have been performed by means of a developed differential optical absorption spectroscopy (DOAS) system based on photodiode array (PDA), during the autumn of 2004. HONO and NO_2 were simultaneously identified by their characteristic absorption bands in the spectral region between 337 nm and 372 nm with high sensibility and time resolution. The concentrations of HONO exhibit obviously diurnal variation with a nocturnal maximum and a daytime minimum. The highest HONO value up to 11.8 $\mu g/m^3$ was observed during the night of 2/3 September. Possible sources of the observed HONO were discussed. Good correlation to NO_2 indicates that NO_2 is a main source component. The measurement also shows direct emission of HONO is an important source in strongly polluted urban area.

Keywords: atmospheric measurements; HONO; NO_2; DOAS; source

Introduction

Nitrous acid (HONO) plays an important role in the polluted atmosphere, since HONO photolysis is a direct source of hydroxyl(OH) radical:

$$HONO+h\upsilon(290\ nm<\lambda<400\ nm) \longrightarrow NO+OH \quad (R1)$$

OH radical is a key intermediate for all the photochemical processes in atmospheric chemistry.

The OH radical may subsequently attack organics starting a chain photoxidation, which leads to the production of ozone, peroxyacetyl nitrate (PAN) and many other secondary pollutants (Platt *et al.*, 1980; Pitts *et al.*, 1984). Therefore the photolysis of HONO enhances the rate of photochemical smog formation. Furthermore, HONO has been suggested to be a potential carcinogenic agent: it reacts rapidly with gaseous secondary amines in air to form nitrosamines (Tuazon *et al.*, 1978; Pitts *et al.*, 1978). Despite this importance, HONO is one of the least researched species in inorganic chemistry (Lammel and Cape, 1996). The formation mechanism of HONO and its atmospheric chemistry are still unclear (Gu *et al.*, 2002; Finlayson-Pitts *et al.*, 2003; Kleffmann *et al.*, 2004). To our knowledge, only few studies concerned the concentrations of HONO in urban areas of China, there is still a lack of information on HONO nighttime sources.

Several important trace gases were first measured with differential optical absorption spectroscopy (DOAS), e.g., HONO, OH, NO_3, BrO, ClO in the troposphere (Stutz and Platt, 1996). DOAS technique can provide realistic, automated and enduring measurement capabilities for multi-species large-area monitoring and avoid sample preparation difficulties characteristic of many point monitoring techniques. Therefore it is widely used as a powerful technique in atmospheric research. The aim of this work was to evaluate the atmospheric level of HONO with a developed DOAS system and discussed the nighttime possible sources of HONO in urban areas of Beijing. In addition, the correlation between HONO and NO_2 were considered.

1 Experimental setup

1.1 Description of the DOAS system

DOAS technique was pioneered by Perner and Platt(1979) in the later 1970s and now was developed into a very useful method for the detection of atmospheric trace gases. The concentrations of trace species in the atmosphere are measured by recording their differential absorption of an UV-Visible light source over a path length of 100 m to several kilometers. According to the characteristic absorption structure and amount of each molecule, multi-pollutants can be measured simultaneously and quantitatively. Atmospheric HONO was first measured by DOAS system with slotted disk (SD) detector (Perner and Platt, 1979). According to the advantages of the built-in multiplexing capability and its long light integration times, PDA has improved DOAS technique compared with SD detector. Fig.1 shows the home-made DOAS system used for the investigation of atmospheric HONO. Light from a high-pressure xenon lamp is collimated by the

Foundation item: The Key Project of Chinese Academy of Sciences (No. KJCX2-SW-H08) and the Hi-Tech Research and Development Program(863) of China(No. 2002AA641020)

combined sending-receiving Cassegrain telescope and sent through the atmosphere. After being absorbed and scattered by trace gases and particles, the light is returned precisely back to the telescope by a retroreflector array. The reflected light is collected by the telescope and led through an optical fiber guide to spectrometer. The dispersed light was recorded by a 1024-element diode array. A stepper motor controller controls two motors. The first motor is used to switch a shutter actuator from reference mode to measure mode. The second carries a filter wheel which can be done in two ways. First, in order to reduce the stray light of spectrograph a filter (ZWB3) is used to take spectra in the UV between 303—375 nm. Second, a baffle is used to record background spectra. The whole system is controlled by a computer via a standard parallel interface.

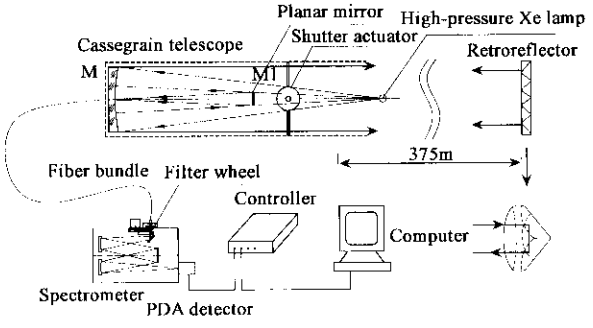

Fig.1 Schematic view of a DOAS instrument used to measure HONO and NO_2

1.2 Measurement site

The DOAS system was placed on the roof of the apartment building for the graduate student (IAP, CAS), at a height of 20 m above the ground. A busy building site was nearby. To the northeast of the measurement site was a park area with trees. The retroreflector array was put on the roof of the office building of Institute of Geology China Earthquake Administration. The light path of 375 m (one way) covered a residential area with low buildings. The light path ran approximate vertical to the heavy traffic route of Badaling freeway, which was located about 300 m to the west. Most of the emission of air pollutants in the vicinity of the measurement site arose mainly from traffic and the building site.

2 Measurement routines and data analysis procedure

For the identification of HONO and NO_2 the spectral range was 337—372 nm where HONO exhibits two distinct absorption peaks at 354.1 and 368.1 nm, which have a differential absorption cross section of 5.0×10^{-19} and 4.5×10^{-19} cm^2/mol(Bongartz *et al.*, 1994), respectively. In order to obtain an optimized measurements quality, a mercury lamp spectrum for the spectrometer calibration and the Xe lamp spectrum("zero path") were taken everyday. In an atmospheric HONO measurement sequence, an air spectrum of correct wavelength regions with single scan was first measured and according to the intensity of preceding air spectrum the integration time of PDA was adjusted to an empirical value that the signal from the interesting part of the spectrum corresponding to about 75% of the maximum level for the ADC, and then a raw air spectrum and a background spectrum with the same scan numbers and integration time were recorded. In high-pressure situations with clean sky the spectrum per 30 s which approximately 30 data added up was recorded at a spectral resolution of 0.42 nm in an interval of 72 nm. Sulfur dioxide (SO_2), ozone (O_3), formaldehyde (HCHO), NO_2 and HONO can be measured simultaneously in this broad spectral range. Here we only concentrate on the situation of NO_2 and HONO. The atmospheric spectrum is evaluated according to the algorithms described by Platt and Stutz(Platt and Perner, 1983; Stutz and Platt, 1996). The background spectrum caused by electronic offset and the dark leakage current of PDA was first subtracted from the respective atmospheric spectra. After being corrected the background spectra, each spectrum was divided by the lamp spectrum which previously corrected background spectra to remove a part of the diode sensitivity and the broadband structure. Following application of high pass filtering, logarithm and smoothing in turn, the resulting spectrum was then further analyzed by a combined linear/nonlinear least squares procedure by fitting reference spectra (or differential absorption cross section) of trace gases and the spectral structure of the lamp simultaneously. It is noticed that the reference spectra must be recorded in the same way as the atmospheric spectrum, using the same width of the entrance slit, etc., and evaluated with the same parameters. The concentrations of the respective species were calculated from the scaling factors of the reference spectra and the differential absorption cross section. Fig.2 shows the spectral signatures of the absorbers retrieved in the wavelength range 337—372 nm. Fig.2a shows the raw atmospheric spectrum recorded by PDA. In Fig.2b the differential optical density spectrum (thin curve) obtained from the atmospheric spectrum (a) is shown together with a reference spectrum of NO_2 (thick curve) scaled to represent 111.0 $\mu g/m^3$ (59 ppb) over the 750 m light

path. To evaluate the mixing ratio of HONO, nearby and overlapping bands arising from NO_2 are eliminated by subtraction of a suitably weighted NO_2 reference spectrum. Fig.2c shows the atmospheric spectrum after subtraction of the NO_2 reference spectrum together with a reference spectrum of 7.7 $\mu g/m^3$ (4 ppb) HONO (thick curve). The absorption structure of HONO can clearly be identified. After the removal of all known absorption structures from the atmospheric spectrum(a), the final residual is shown in Fig.2d. The residual absorption structures (d) might be related to the electronic noise of the instrument or other unknown absorbers. The trace-gas detection limit (in terms of optical density) given by the peak-to-peak is about 8×10^{-4}, which, for the 750 m path, results in a detection limit of about 1.7 $\mu g/m^3$ for NO_2 and about 0.7 $\mu g/m^3$ for HONO.

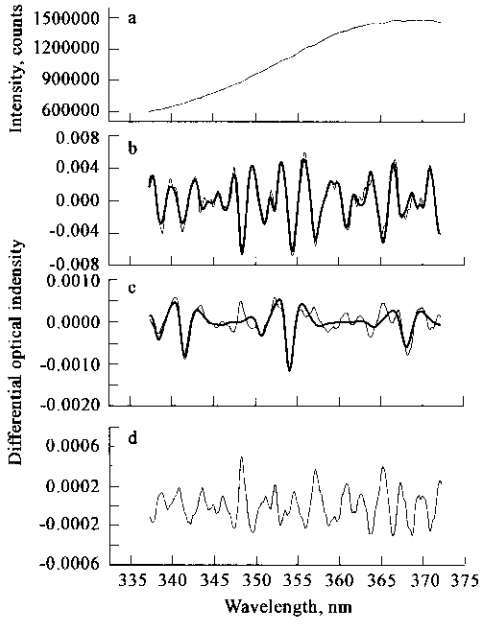

Fig.2 Retrieved NO_2 and HONO absorptions from spectra recorded during the Beijing experiments on 30 August 2004
a. atmospheric spectrum; b. differential spectrum (thin curve) compared with a reference spectrum of 111.0 $\mu g/m^3$ NO_2 (thick curve); c. the atmospheric spectrum after subtraction of the NO_2 reference spectrum is shown in(c) together with an HONO reference spectrum of 7.7 $\mu g/m^3$(thick curve); d. the residual spectrum of about 8×10^{-4}(the peak-to-peak value) after fitting of all the trace gases

3 Results and discussion

3.1 Time series of NO_2 and HONO

DOAS measurements of NO_2 and HONO were performed in two weeks from Aug. 24 to Sep. 5, 2004. Fig.3 shows the time series of the concentrations of NO_2 and HONO. Due to the system malfunction and other reasons, DOAS data shows several gaps in Fig.3. The diurnal variation as well as the correlation of both gases can be clearly seen. NO_2 concentrations ranged between 9.6 $\mu g/m^3$(5 ppb) and 159.9 $\mu g/m^3$(85 ppb), with a daytime minimum during large actinic flux and a nighttime maximum. Because of the rapid photolysis NO_2 level showed very low around 12:00. Most nights showed high NO_2 value before midnight and low values after midnight. The increase of NO_2 may be the consequences of the continuous NOx emission from vehicle traffic, the reaction of O_3 with NO, the decrease of the boundary layer and missing photolysis of NO_2 from sunset. Due to the consumption of O_3, low traffic density and other removal paths of NO_2, the concentrations of NO_2 decreased after midnight. HONO levels ranged between below the detection limit of 0.7 $\mu g/m^3$ and a maximum of 11.8 $\mu g/m^3$(6.1 ppb). HONO started to increase right after sunset and had two peaks in midnight and the early morning, respectively. The concentration levels of HONO are in good agreement with the measurements observed by other workers under moderately to strongly polluted urban conditions (Harris *et al.*, 1982; Sjödin, 1988; Andrés-Hernández, 1996; Alick *et al.*, 2002). Due to the different measurement situation and measurement instrument, our results of HONO show higher 1 h average about 10.4 $\mu g/m^3$ compared with the highest 1 h average of about 5 $\mu g/m^3$ which was observed by means of SJAC-MOBIC(steam jet aerosol collector combined with mobile ion chromatograph system) in Peking University campus, 2000 (Zhou *et al.*, 2002).

In the following we will concentration on two periods. One is from the midnight of 25 August to the morning of 27 August, another is from the midnight of 1 September to the morning of 3 September 2004.

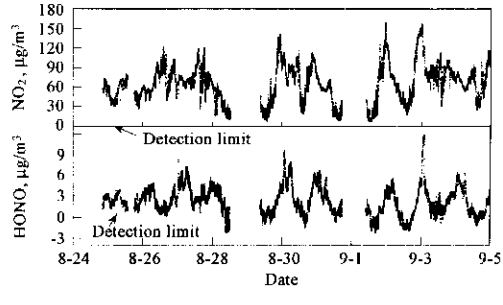

Fig.3 Time series of HONO and NO_2

3.2 Diurnal variation of HONO

Fig.4 shows the variation of HONO and NO_2 concentrations during these two periods. In order to compare with the results made by other workers, we use mixing ratios (ppb) to express the trace gases concentrations. HONO exhibited a typical diurnal pattern with nighttime maximum, and lesser peak during the morning rush hour, has been observed in

(a) and (b) of Fig.4. In contrast with (b), the individual data points of HONO in (a) during solar radiation (between 5:00 and 20:00) were only 6.5% below the detection limit, but 80.8% for (b). Because of the attenuation of NO_2 photolysis, it is easy to notice that the concentrations of NO_2 during the midday in (a) are much higher than others in (b). Due to a dense cloud cover and the aerosol and particles emitted by traffic or the building site, which may attenuate the incoming solar radiation, the photolysis rates during the morning hours of 26 August stayed low until 12:00. HONO mixing ratio was up to 1.2 ppb at 14:59. Owing to the fast photolysis into OH radical(Reaction(R1)), the life-time of HONO at 12:00 is about 9.5 min under clear sky conditions (Alicke *et al.*, 2002). When photolysis ceases, concentrations of HONO gradually increase after sunset. The main mechanisms in the primary production of the chain-initiating OH radical involve the photolysis of O_3, aldehydes(especially HCHO) and HONO. Although the photolytic steps involve O_3 is the dominant mechanism of OH formation, our measurements(Fig.5) show the concentrations of O_3 in the early morning was very low due to the consumption by the reaction with NO emitted from vehicle traffic. Despite HCHO photolysis begins earlier in the morning and lasts longer in the evening, the HCHO concentrations(below 10 ppb at 6:00) were relatively low during that time. Both photolysis pathways including O_3 and HCHO for OH production closely follow actinic flux. The results of measurements and simulation show the maximum of radical production from HCHO photolysis was around noon but the maximum for O_3 photolysis was later in the day (Winer, 1985; Schiller *et al.*, 2001; Harris *et al.*, 1982; Alick *et al.*, 2002, 2003). Furthermore, the rate of radical production from HCHO by photolysis is much less than that from HONO for equal concentration(Platt *et al.*, 1979). From our observation HONO is the greatest important OH source in the early morning, even significant in cloudy condition.

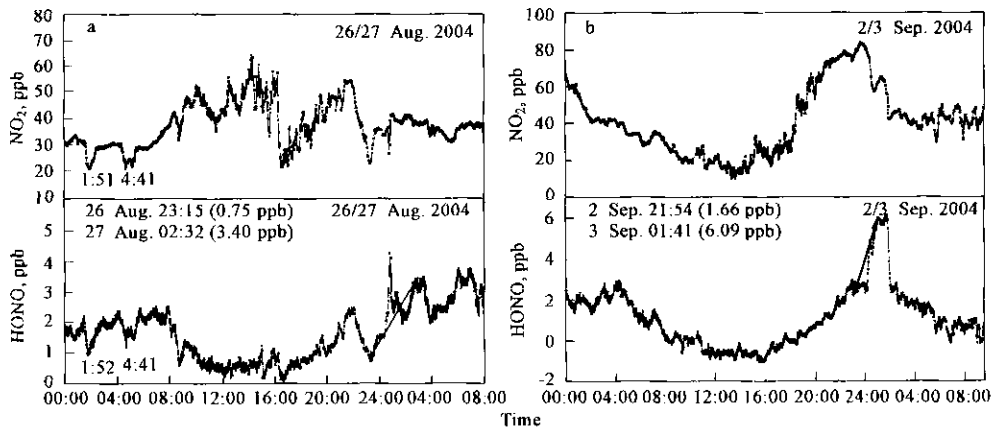

Fig.4 Behavior of [NO_2] and [HONO] during two periods (26/27 August, 2/3 September, 2004). The first period was characterized by low sunlight intensity and low visibility. The second period was characterized by cloudy sky with high relative humidity(>80%) after midnight of 3 Sep.

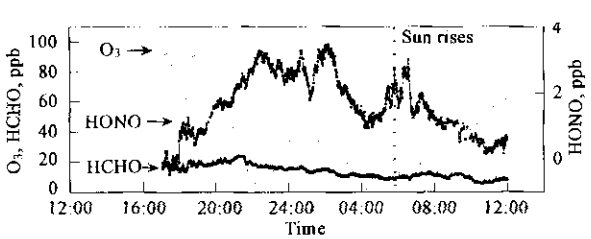

Fig.5 Concentrations of O_3, HCHO and HONO in the early morning

3.3 Correlation between HONO and NO_2

NO_2 is known to be an important precursor for the formation of HONO or have a common source. The concentrations of HONO and NO_2 were found to be highly correlated. The highest HONO concentration was observed on the nights with high NO_2(Fig.4). Fig. 6 presents the correlation of HONO and NO_2 for the night of 25/26 Aug. and the variation of HONO/NO_2 during two nights of 25/26 Aug. and 2/3 Sep. An average HNO_2/NO_2 ratio of 8.4% was calculated from the data of Fig.6a. This ratio is within the wide range between approximately 2% and 10% which was observed in many other studies (Platt, 1986; Allegrini and Febo, 1995; Lammel and Raes, 1996; Febo *et al.*, 1996; Alick *et al.*, 2002, 2003). A total of 762 individual HONO-NO_2 data points (from 21:00 to 8:00) exhibit a clear positive correlation for R=0.77. Similarly to NO_2, two lower mixing ratios of HONO (Fig.5a) appeared at 1:51 and 4:41 during the night of 25 and 26 Aug. One can expect that if HONO was formed from NO_2, there would be a delay between the peaks of NO_2 and HONO because of the time required for HONO formation. The observation of constant

HONO-to-NO_2 ratios can be explained by a receptor site situation. These two pollutants have a common emission source. As stated by Lammel *et al.*, well mixed pollutant concentrations are more dominated by advection from an upwind source rather than local emission, the concentrations of NO_2 and HONO are strongly influenced by the transport times since emission of the precursor. As wind speed dropped, a shift from the situation of "a receptor site" to "a smog chamber" occurred. In case of "a smog chamber" pollutants accumulate through direct emission or chemical transformation processes and inefficiently mix with outsider air at low wind speeds, and is comparable to a smog chamber during filling. In this case NO_2 lost during the night while HONO was formed, the increasing HONO-to-NO_2 ratios would be observed(Fig.6b).

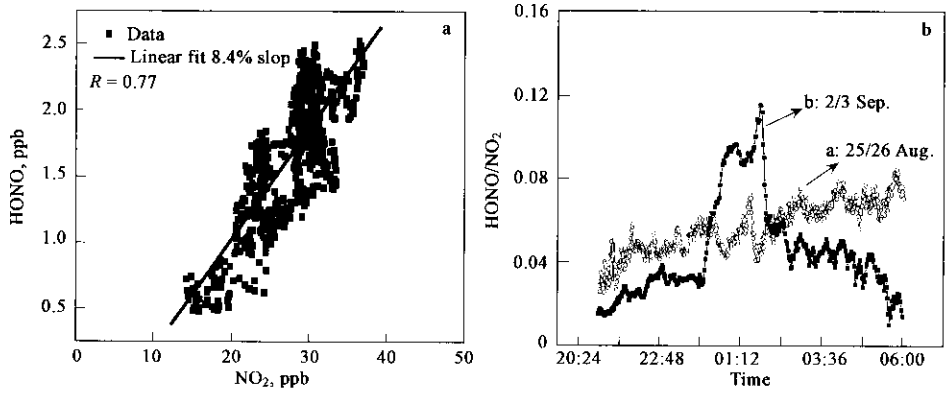

Fig.6 Correlation between HONO and NO2 for the night 25/26 August 2004. An average slope of 8.4% can be derived from the data (a). Variation of HONO/NO2 during the two nights of 25/26 Aug. and 2/3 Sep.(b)

3.4 Possible nighttime sources of HONO

To date, the mechanism for the observed nighttime formation of HONO is still poorly understood. The following formation pathways are suggested as the sources of HONO:

(1) Direct emission. HONO is a primary product of emission from combustion sources. Early investigation by Kirchstetter *et al.* (1996) in a traffic tunnel in the United States shows HONO/NO_2 ratio of 0.3%. More recently, a higher ratio of about 0.65% was observed in European(Kurtenbach *et al.*, 2001).

(2) Homogeneous gas-phase reactions. Reaction (R2) was considered as the most important homogeneous reaction forming HONO:

$$NO+OH \rightarrow HONO \quad (R2)$$

(3) Heterogeneous reaction. The following stoichiometry involving nitrogen oxides and water vapor have been suggested (Notholt *et al.*, 1992; Calvert *et al.*, 1994; Harrison *et al.*, 1994; 1996; Ammann *et al.*, 1998; Reisinger, 2000; Finlayson-Pitts *et al.*, 2003):

$$NO + NO_2 + H_2O \xrightarrow{surface} 2HNO_2 \quad (R3)$$

$$2NO_2 + H_2O \xrightarrow{surface} HNO_2 + HNO_3 \quad (R4)$$

To investigate the direct emission of HONO, the HONO/NO_2 ratio of 0.65% for direct emissions by cars was used to calculate the $HONO_{em}$-to-HONO ratio:

$$R_{HONO_{emission}/HONO} = \frac{0.0065 \times [NO_2]}{[HONO]} \quad (1)$$

The individual data points between 16:00 and 6:00 during the night of 26 and 27 Aug. were chosen to confirm the situation of the direct emission for the low sunlight intensity in daytime and low wind speeds throughout the night. Here, we used $[NO_2]$ as $[NO_x]$ (NO_x=NO+NO_2) to calculate direct HONO emission due to high ozone concentrations during this night (Fig.7a), and NO could well be consumed by O_3. Fig. 7b shows the variation of $HONO_{em}$/HONO ratio during this night. The highest $HONO_{em}$/HONO ratio of 93% was observed at about 16:50, which is consistent with the onset of the traffic in the afternoon. It appears that during the first half of the night the HONO levels originate from the direct emission, but for the second half of the night its contribution is not significant.

Homogeneous reaction (R2) plays a role during the day when OH and NO concentrations high, but it is not likely to account for the observed nighttime formation of HONO since it is balanced by the photolysis of reaction (R1) during the day. In the absence of direct HONO sources, the steady state mixing ratio of HONO around noon can be observed from Fig.4b. According to the literature OH concentrations are usually low during the night, and NO concentrations are also low which can be derived

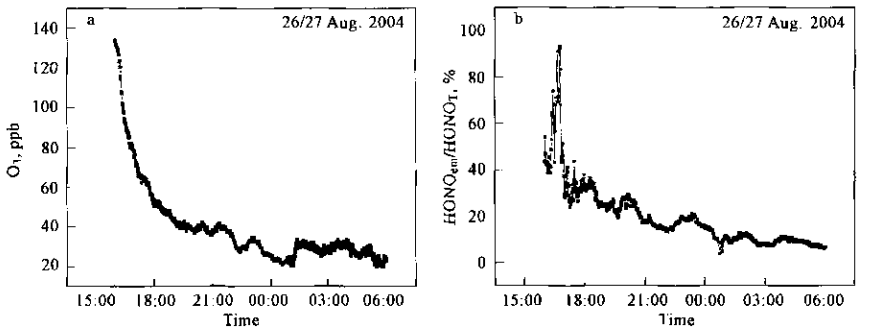

Fig.7 The variation of O_3 mixing ratios during the night of 26/27 Aug. 2004 (a); the variation of $HONO_{em}/HONO$ ratio during the night of 26/27 Aug. 2004 (b)

from the nighttime ozone concentrations. R2 may be significant around sunset, but the fact that there would be other mechanisms for the dominant sources of nighttime HONO formation exists.

Heterogeneous reactions R3 and R4 can proceed on the ground surface or aerosol. Many laboratory and field studies combined with our observations suggest that R3 is not important as the source of HONO by the reason of low NO or even absence. It seems that the reaction involving NO_2 and water vapor may be the major contributor to HONO formation. Here, we use a method described by Alicke *et al.*(2002) to estimate the conversion frequency from NO_2 into HONO during the two nights of 26/27 Aug. and 2/3 Sep. The average nighttime conversion frequency was determined by:

$$\overline{F}_{\mathrm{HONO,night}} = \frac{[\mathrm{HONO}]_{(t_2)} - [\mathrm{HONO}]_{(t_1)}}{(t_2 - t_1)[\overline{\mathrm{NO_2}}]_{\mathrm{night}}} \qquad (2)$$

The calculated values were about 0.020 and 0.025 (ppb HONO)/ (h (ppb NO_2)) respectively. As compared with the results of (0.012 ±0.005) (ppb HONO)/(h(ppb NO_2)) calculated by Alicke, our value of the night of 2/3 Sep. is higher. The NO_2 and HONO increased slightly from sunset to about midnight with high levels. In contrast to NO_2, the concentration of HONO increased rapidly only from about 0:10 and reached a peak of 6.1 ppb at 1:40. Most results of laboratory studies show that the formation of HONO is first order in NO_2, but the rate of R4 is too slow to explain the observed HONO formation. The surface in nature is actually more complex than the surface(e.g. Teflon, PFA, Pyrex, Quartz, and Glass) used in experimental studies. Ammann *et al.*(1998) found that the heterogeneous production of HONO from NO_2 on fresh suspended soot particles proceeds 10^5 to 10^7 times faster than on previously studied surfaces, indicating that fresh soot may have a considerable effect on the chemical reactions occurring in polluted air. It is apparent that HONO formation depends not only on the available surface, but also on the composition of the surface (Stutz *et al.*, 2004). The laboratory studies and the heterogeneous nature of the reaction were shown by increase of the conversion frequency with the surface to volume ratio (Finlayson-Pitts *et al.*, 2003; Kleffmann *et al.*, 1998; Svensson *et al.*, 1987). During the nighttime, the boundary layer is separated from the ozone reservoirs in the troposphere. When the wind went down, the pollutants and the particles emitted from the ground were trapped in a diminished volume. At measurement site, with a busy building site and the heavy traffic much closer, abundant suspended soot particles and mineral dust could be supply by the areas which can provide large surface areas for HONO formation. Although the mechanism of water vapor and NO_2 involving in the formation of HONO is still unclear, many field observations and laboratory measurements suggest that the water vapor plays a more important role in the reaction. The results observed by Stutz stutz *et al.* (2004) show that [HONO]/[NO_2] ratios between 10 and 30% RH do not exceed 0.04, while values of up to 0.09 were observed at higher RH. The high conversion frequency of the night of 2/3 Sep. may be caused by the chemical transformation of NO_2 at high relative humidity(>80%) in the low nighttime boundary layer. It is interesting to notice that HONO declined rapidly after reaching the maximum at 1:40. This may be explained by the effects of deposition or the change of air masses.

4 Conclusions

Measurements of HONO and its precursor NO_2 were obtained in Beijing City during the autumn of 2004, by a developed DOAS system based on PDA. The system showed high sensibility and high time resolution in the spectral range from 337—372 nm for identifying HONO and NO_2. The detection limit is about 1.7 μg/m^3 for NO_2 and about 0.7 μg/m^3 for

HONO respectively over a light path of 750 m.

It is the first time to investigate the nighttime source of HONO in China. From our results, as a potential consequence of the combination of high relative humidity and the decrease of the boundary layer, the highest HONO concentration of reaching about 11.8 $\mu g/m^3$ with an average conversion frequency of 0.025 (ppb HONO)/ (h (ppb NO_2)) was observed during the night of 2/3 Sep. The nighttime source of HONO was discussed, and the heterogeneous reaction involving NO_2 and water vapour occurred on the ground or aerosol may be the main contributor for the nocturnal formation of HONO. The concentrations of HONO and NO_2 were found to be highly correlated, which is consistent with other studies. This result also implies that the contribution of direct emission of HONO was significant during the first half of night.

Acknowledgments: Special thanks are given to Prof. An Jun-ling, Institute of Atmospheric Physics, CAS, for the help in establishing the measurement site.

References:

Alicke B, Platt U, Stutz J, 2002. Impact of nitrous acid photolysis on the total hydroxyl radical budget during the Limitation of Oxidant Production/Pianura Padana di ozone study in Milan[J]. J Geophys Res, 107(D22): 8196.

Alicke B, Geyer A, Hofzumahaus A *et al.*, 2003. OH formation by HONO photolysis during the BERLIOZ experiment [J]. J Geophys Res, 108(D4): 8247.

Allegrini I, Febo A, 1995. Role of nitrous acid on the oxidation processes in the Mediterranean urban areas [J]. Ann Chim, 85 (7/8): 471- 485.

Ammann M, Kalberer M, Jost D T *et al.*, 1998. Heterogeneous production of nitrous acid on soot in polluted air masses [J]. Nature, 395: 157- 160.

Andrés-Hernández M D, Notholt J, Hjorth J *et al.*, 1996. A DOAS study on the origin of nitrous acid at urban and non-urban sites [J]. Atmos Environ, 30: 175—180.

Bongartz A, Kames J, Schurath U *et al.*, 1994. Experimental determination of HONO mass accommodation coefficients using two different techniques[J]. J Atmos Chem, 18: 149- 169.

Calvert J G, Yarwood G, Dunker A M, 1994. An evaluation of the mechanism of nitrous acid formation in the urban atmosphere[J]. Res Chem Intermed, 20(3/5): 463 -502.

Febo A, Perrino C, Allegrini I, 1996. Measurement of nitrous acid in Milan, Italy, by DOAS and diffusion denuders [J]. Atmos Environ, 30: 3599 —3609.

Finlayson-Pitts B J, Wingen L M, Sumner A L *et al.*, 2003. The heterogeneous hydrolysis of NO_2 in laboratory systems and in outdoor atmospheres: An integrated mechanism [J]. Phys Chem Chem Phys, 5: 223—242.

Gu H, Zhou X L, Deng G H *et al.*, 2002. Measurements of atmospheric nitrous acid and nitric acid[J]. Atmos Environ, 36: 2225- 2235.

Harrison R M, Kitto A M N, 1994. Evidence for a surface source of atmospheric nitrous acid[J]. Atmos Environ, 28: 1089—1094.

Harrison R M, Peak J D, Collins G M, 1996. Tropospheric cycle of nitrous acid[J]. J Geophys Res, 101: 14429- 14439.

Harris G W, Carter W P L, Winter A M *et al.*, 1982. Observations of nitrous acid in the Los Angeles atmosphere and implications for prediction of ozone-precursor relationships [J]. Environ Sci Technol, 16: 414 -419.

Kirchstetter T W, Harley R A, Littlejohn D, 1996. Measurement of nitrous acid in motor vehicle exhaust [J]. Environ Sci Technol, 30: 2843—2849.

Kleffmann J, Becker K H, Wiesen P, 1998. Heterogeneous NO_2 conversion processes on acid surfaces: Possible atmospheric implications[J]. Atmos Environ, 32(16): 2721—2729.

Kleffmann J, Benter T, Wiesen P, 2004. Heterogeneous reaction of nitric acid with nitric oxide on glass surface under simulated atmospheric conditions[J]. J Phy Chem A, 108: 5793—5799.

Kurtenbach R, Becker K H, Gomes J A G *et al.*, 2001. Investigations of emissions and heterogeneous formation of HONO in a road traffic tunnel[J]. Atmos Environ, 35: 3385- 3394.

Lammel G, Cape J N, 1996. Nitrous acid and nitrite in the atmosphere [J]. Chem Soc Rev, 25(5): 361—369.

Notholt J, Hjorth J, Raes F, 1992. Formation of HNO_2 on aerosol surfaces during foggy periods in the presence of NO and NO_2[J]. Atmos Environ, 26A: 211—217.

Perner D, Platt U, 1979. Detection of nitrous acid in the atmosphere by differential optical absorption[J]. Geophys Res Lett, 6: 917—920.

Pitts J N Jr, Grosjean D, van Cauwenberghe K A *et al.*, 1978. Photooxidation of aliphatic amines under simulated atmospheric conditions: formation of nitrosamines, nitramines, amides and photochemical oxidant[J]. Envir Sci Technol, 12: 946—953.

Pitts J N Jr, Biermann H W, Winer A M *et al.*, 1984. Spectroscopic identification and measurement of gaseous nitrous acid in dilute auto exhaust[J]. Atmos Environ, 18: 847—854.

Platt U, Perner D, Pätz H, 1979. Simutanous measurement of atmospheric CH_2O, O_3 and NO_2 by differential optical absorption [J]. J Geophys Res, 84: 6329—6335.

Platt U, Perner D, Harris G W *et al.*, 1980. Observations of nitrous acid in an urban atmosphere by differential optical absorption [J]. Nature, 285: 312—314.

Platt U, Perner D, 1983. Measurements of atmospheric trace gases by long path differential UV/visible absorption spectroscopy[M]. In: Optical and laser remote sensing techniques (Killinger D. K., Mooradian A. ed.). Heidelberg: Springer-Verlag. 97- 105.

Platt U, 1986. The origin of nitrous acid and nitric acid in the atmosphere(Jaeschke W. ed.). New York: Springer-Verlag. 299—319.

Platt U, 1994. Differential optical absorption spectroscopy (DOAS), air monitoring by spectroscopic techniques (Sigrist M. W. ed.)[M]. Chemical Analysis Series. John Wiley & Sons, Inc. 127:27—84.

Reisinger A R, 2000. Observations of HNO_3 in the polluted winter atmosphere: possible heterogeneous production on aerosols [J]. Atmos Environ, 34: 3865—3874.

Schiller C L, Locquiao S, Timothy J J *et al.*, 2001. Atmospheric measurements of HONO by tunable diode laser absorption spectroscopy [J]. Journal of Atmospheric Chemistry, 40: 275—293.

Sjödin Å, 1988. Studies of the diurnal variation of nitrous acid in urban air[J]. Environ Sci Technol, 22: 1086—1089.

Stutz J, Platt U, 1996. Numerical analysis and estimation of the statistical error of differential optical absorption spectroscopy measurements with least-squares methods[J]. Applied Optics, 35 (30): 6041—6053.

Stutz J, Alicke B, Ackermann R *et al.*, 2004. Relative humidity dependence of HONO chemistry in urban areas [J]. J Geophys Res, 109: D03307.

Svensson R, Ljungström E, Lindqvist O, 1987. Kinetics of the reaction between nitrogen dioxide and water vapour [J]. Atmos Environ, 21(7): 1529—1539.

Tuazon E C, Winer A M, Graham R A *et al.*, 1978. Fourier transform infrared detection of nitramines in irradiated amine-NO_x system [J]. Envir Sci Technol, 12: 954—958.

Winer A M, 1985. Air pollution chemistry [M]. In: Handbook of air pollution analysis (M. Harrison, R. Perry, ed.). 2nd ed. London: Chapman and Hall.

Zhou F M, Shao K S, Hu M *et al.*, 2002. Concentration of aerosol and related gas in Beijing[J]. Environmental Science, 23(1): 11—15.

(Received for review February 3, 2005. Accepted April 19, 2005)